Analysis of Dielectric and Conductive Dispersion above T-g in Glass-Forming Molecular Liquids

ARTICLE *in* THE JOURNAL OF PHYSICAL CHEMISTRY B · NOVEMBER 2008

Impact Factor: 3.3 · DOI: 10.1021/jp805535w · Source: PubMed

1 AUTHOR:

James Macdonald
University of North Carolina at Chapel Hill
203 PUBLICATIONS **7,844** CITATIONS

SEE PROFILE

ARTICLES

Analysis of Dielectric and Conductive Dispersion above T_g in Glass-Forming Molecular Liquids

J. Ross Macdonald*

Department of Physics and Astronomy, University of North Carolina, Chapel Hill, North Carolina 27599-3255

Received: June 23, 2008; Revised Manuscript Received: July 18, 2008

Dynamics of the nonassociated supercooled liquids *N*-methyl-ε-caprolactam (NMEC) and glycerol in the frequency domain are investigated using full complex-nonlinear-least-squares fitting of immittance spectroscopy data for appreciable temperature ranges above the glass transition. Such fitting, not previously used for these materials, helps to identify physical processes responsible for the data and elements of their common behavior. Several different fitting models were applied to find a physically plausible best-fitting one to distinguish quantitatively between the dielectric effects of dipoles and the conductive effects of mobile ions. The utility of many composite fitting models was investigated, and although a pure conductive-system dispersive (CSD) fitting model led to good but physically unrealistic fits of all data sets, the dielectric-system dispersive (DSD) Davidson−Cole model best fitted the α-dispersion part of the responses. Nevertheless, the series combination of such a DSD model and a separate CSD model (one not associated with electrode effects) was found to yield much better fitting of the data for both materials. Although the CSD model plays somewhat the role of the conventional parallel DSD Johari−Goldstein β-response, it is here in series and arises from mobile impurity-ion effects rather than from dipolar ones. Previous analyses of data of the present and other molecular materials have often involved two DSD models in parallel, but fitting with such a composite model led here to less physically plausible parameter values and ones with appreciably more uncertainties. Surprisingly, the series DSD and CSD composite-model fits led to comparable estimated values of the NMEC and glycerol dielectric strength parameters, as well as to the nearly equal small thermal activation energies of these parameters.

1. Introduction

This work is concerned with approaches for identifying the physicochemical microscopic origins of the dispersed frequency response observed in such liquids as *N*-methyl-ε-caprolactam (NMEC), a low molecular weight nonassociating liquid involving small rigid molecules with predominant van der Waals interactions,[1−3] and glycerol, an ideal H-bonded alcohol.[3−6] For these materials, dispersive effects are particularly interesting in the high-viscosity temperature region just above the glass transition temperature, T_g, about 172 K in NMEC and 185 K in glycerol. In this region, crystallization is surpressed; the material is characterized as glass forming; and its conductivity, associated with mobile impurity ions, is appreciable. A list of acronym definitions and fitting model descriptions is included at the end of this work.

In general, available dispersed immittance response data in the frequency range $0.1 \leq \nu < 10^6$ Hz for the NMEC data and from about 0.01 Hz to nearly 10^9 Hz in glycerol may involve several distinct physical processes: (a) dielectric-system dispersion (DSD) associated with the presence of permanent and/or induced dipoles;[4−7] (b) conductive-system dispersion (CSD) involving a distribution of resistivity relaxation times associated with thermally activated ionic hopping;[8−10] (c) both processes present and each leading to significant dispersed response usually dominant in different frequency regions; and (d) case (c) plus one or more nondispersive relaxation processses. For case (a), it is usually assumed that any observed resistivity is frequency independent in the measured data range and may be represented by its dc value, ρ_0.[1,11,12] Similarly, for (b), one assumes that in this frequency range dipolar and vibratory effects lead to a frequency-independent bulk dielectric constant, $\varepsilon_{D\infty}$, often denoted by just ε_∞. Apparently, composite-model analysis approaches for cases (b), (c), and (d) have not been considered for molecular liquid data prior to the present work.

Because the meanings of the words "relaxation" and "dispersion" have not always been clear or adequately distinguished for temporal and frequency response situations, it is worthwhile to define them for the present work. Although the word "relaxation" has often been employed to mean either dispersion and/or single-time-constant Debye relaxation, here "relaxation" will refer only to a process involving a single relaxation time. In contrast, a dispersive process is one that involves either many discrete individual relaxation times or a continuous distribution of such times, in either case a distribution of relaxation times (DRT). It may be modeled in the time or frequency domain by a single response function involving a characeristic relaxation time, and when its DRT is a Δ function the response involves only a single relaxation time, Debye relaxation response. It follows from the above definitions that such designations as

* Corresponding author. Phone: (919) 967-5005. E-mail: macd@email.unc.edu.

10.1021/jp805535w CCC: $40.75
Published on Web 10/09/2008

"the nonexponentiality of relaxation" necessary imply the presence of dispersion and corresponding deviation from Debye response.

In the time domain, Debye relaxation response is of the form $\exp(-t/\tau_0)$ and leads in the frequency domain to the normalized response $I(\omega) \equiv 1/[1 + i\omega\tau_0]$. Here, $\omega = 2\pi\nu$ is the radial frequency, and τ_0 is the characteristic relaxation time of the response function and is unique for that response. Thus, Debye relaxation is not dispersive. In the frequency domain, immittance spectroscopy involves four related complex-quantity immittance levels, defined as resistivity (or impedance), $\rho(\omega)$; electric modulus, $M(\omega) = i\omega\varepsilon_V\rho(\omega)$; admittance (or conductivity), $\sigma(\omega) = 1/\rho(\omega)$; and dielectric permittivity, often called dielectric constant (even when frequency dependent and complex), $\varepsilon(\omega) = 1/M(\omega) = \sigma(\omega)/(i\omega\varepsilon_V)$, where ε_V is the permittivity of vacuum.

It is important to note that while any formal fitting model may be used for fitting of data expressed at any of the four immittance levels, definition of a model at the dielectric level involves a distribution of dielectric relaxation times, usually associated with dipolar effects, and definition at the resistivity level involves a resistivity DRT, often associated with hopping of mobile ions. Thus, for Debye dielectric relaxation, we may write $\varepsilon_{DebD}(\omega) = \varepsilon_{D\infty} + \Delta\varepsilon/[1 + (i\omega\tau_{D0})]$, where $\Delta\varepsilon \equiv \varepsilon_{D0} - \varepsilon_{D\infty}$, involving the low and high-frequency limiting values of $\varepsilon_{DebD}(\omega)$. Similarly for Debye conductive-system relaxation, $\rho_{DebC}(\omega) = \rho_\infty + \Delta\rho/[1 + (i\omega\tau_{C0})]$, where $\Delta\rho = \rho_{C0} - \rho_{C\infty}$, the low- and high-frequency limiting values of $\rho_{DebC}(\omega)$. In the present work, no dielectric Debye functions will be needed for fitting, so endemic resistive Debye relaxation response will often be denoted here by just Debye.

It is usually found that ρ_∞ is either zero or negligible, the situation for the present materials, but ε_∞ is never negligible for real materials. The subscripts "C" and "D" are used herein to denote conductive or dielectric quantities and "P" or "S" for parallel or series connections of individual models or elements. Note that a resistance or resistivity in parallel with a capacitance or dielectric constant element leads to conductive-system Debye response. In the absence of ρ_∞, it involves the quantities ρ_{CP}, ε_{CP}, and the characteristic relaxation time $\tau_{CP} = \varepsilon_V\varepsilon_{CP}\rho_{CP}$. Similarly for the series connection of ρ_{DS} and ε_{DS}, one obtains a dielectric-system Debye relaxation response of $\varepsilon_{DS}/(1 + i\omega\tau_{DS})$ with $\tau_{DS} = \varepsilon_V\varepsilon_{DS}\rho_{DS}$. More general conductive-system dispersive response involves a weighted (i.e., a DRT) sum or integral of resistive and dielectric elements in parallel,[9] and dielectric-system dispersive response involves a weighted sum or integral of resistive (effective loss parameter) and dieletric elements in series, defined at the dielectric level.

Athough electromagnetic theory precludes distinguishing between dielectric and mobile-charge bulk effects by means of external measurements, such as those of immittance spectroscopy, the present materials are molecular, and thus choice (a) is the conventional and natural one. On the other hand, ionic motion in ion-conducting glasses has been shown to lead to type (b) CSD response that is well modeled by a continuous-time, random-walk hopping model associated with stretched-exponential temporal behavior.[8,13,14] Finally, if both processes were simultaneously present as in case (c), one might expect that each could lead to a separate but possibly unresolved dispersion peak. Alternatively, a single dispersion process and a relaxation (Debye) process might be present. Although all of the above types of response could potentially play some role in the data for the present materials, not all are necessarily physically plausible for them.

A previous detailed fitting study[15] surprisingly showed that synthetic type (a) dispersed dielectric frequency response data with some frequency-independent conductivity (i.e., involving no resistivity relaxation times leading to dispersed response in the measured frequency domain) could be well fitted by a type (b) ionic hopping model with a frequency-independent $\varepsilon_{D\infty}$, and vice versa. It was suggested there that some discrimination between the two dispersion types might be possible if data for a range of temperatures were available. The present study shows, however, that physical considerations are necessary as well to achieve meaningful discrimination for the present molecular liquids.

Yet why might it matter? A reader of an earlier version of the present work stated that "any dielectric expert" would conclude from the NMEC data that it represents "a conventional dipolar relaxation scenario with some ionic conductivity due to impurity." Note the use of the word "relaxation" here. Another reader suggested that measurements in the time domain would allow one to distinguish between dipolar and mobile charge bulk effects because on the application of a step electric field the former would store energy and the latter would dissipate energy without limit. Because there are no ideal dielectric materials and all show some impurity-ion conductivity, this argument is inappropriate, and dielectric experts who reach conclusions based just on the plotted shape of data curves, or even on approximate fits of the data perhaps assuming simple dipolar relaxation ab initio, may thereby be ignoring the complexity of real data.

Section 2 defines the individual and composite fitting models used herein, including parts that represent possible electrode effects, dielectric dispersion, and conductive-system dispersion. Only two different dispersive models are used, but each involves separate dielectric and conductive forms. Section 3 summarizes the detailed data and fit results found for the present supercooled liquids, and section 4 lists conclusions that follow from the fitting results and analyses.

2. Fitting Models

2.1. A General Fitting Model Transformation. Although there are a large number of possible models that have been used for representing bulk dispersion, for simplicity I shall be concerned here with only a few, most of which have been widely employed in past work and might be pertinent for the present data sets. Several different DSD models have been used in the past to fit the α-dispersion region of the dielectric-level frequency response of glass-forming molecular liquids. Yet often only the imaginary part of the data, expressed at the dielectric level, $\varepsilon''(\omega)$, has been considered, and rarely is the adequacy of several different models quantitatively compared for the same data sets. It is also rare that complex fits of full data sets have been carried out. Therefore, the present work involves complex fits of all $\varepsilon(\omega)$ data for several possibly appropriate models of DSD, CSD, and mixed character.

As already mentioned and demonstrated, a given dispersive frequency-response model may be defined either at the resistivity level, involving a distribution of resistivity relaxation times, or at the complex dielectric constant level, then involving a distribution of dielectric permittivity relaxation times. To distinguish types of models, let the subscript k take on the values D, for DSD models, and 0 for a comparable type of CSD model. Next, in terms of the normalized general response function, $I_k(\omega)$, which satisfies $I_k(0) = 1$ and $I_k(\infty) = 0$, one may write for DSD situations, $\varepsilon_D(\omega) = \varepsilon_{D\infty} + \Delta\varepsilon_D I_D(\omega)$, where $\Delta\varepsilon_D \equiv \varepsilon'_D(0) - \varepsilon'_D(\infty)$, the dielectric strength function, hereafter

designated by just $\Delta\varepsilon$, and we denote $\varepsilon'_D(0)$ and $\varepsilon'_D(\infty)$ by ε_{D0} and $\varepsilon_{D\infty}$, respectively. Similarly, for the $k = 0$ CSD situation, $\rho_C(\omega) = \rho_{C\infty} + \Delta\rho_C I_0(\omega)$, where $\Delta\rho_C \equiv \rho'_C(0) - \rho'_C(\infty)$, with $\rho'_C(0) \equiv \rho_{C0}$ and $\rho'_C(\infty) \equiv \rho_{C\infty}$. In the usual situation of $\rho_{C\infty}$ negligible or zero, $\Delta\rho_C$ is equal to ρ_{C0}.

Besides the $k = 0$ CSD type of response, another important one exists that may be derived from such response and will be identified by the $k = 1$ choice. In 1973, it was shown separately from both macroscopic[16] and continuous-time, random-walk microscopic[13,14] considerations that for a CSD situation a new frequency-response model, $\rho_{C1}(\omega)$, could be derived from the $k = 0$ $\rho_C(\omega)$ one. Few other important CSD fitting models besides the present $\rho_{C1}(\omega)$ one have been derived from both microscopic and macroscopic analyses.

With $\rho_{C\infty}$ negligible, the complex modulus function associated with $\rho_{C1}(\omega)$ is $M_{C1}(\omega) \equiv i\omega\varepsilon_V\rho_{C1}(\omega)$, and the transformation from a $k = 0$ model to a $k = 1$ one is then given by[8,9,14,16]

$$M_{C1}(\omega) = i\omega\varepsilon_V\,\rho_{C0}\,I_1(\omega) = [1 - I_{01}(\omega)]/\varepsilon_{C1\infty} \qquad (1)$$

where we do not distinguish between $k = 0$ and $k = 1$ ρ_{C0} quantities but use the same symbol for both, with $\sigma_{C0} = 1/\rho_{C0}$. The 01 subscript in eq 1 indicates that, although the $k = 0$ $I_0(\omega)$ function involves its usual shape parameter, the value of this parameter is to be determined by fitting data with the $\rho_{C1}(\omega)$ model, not with the $\rho_{C0}(\omega) \equiv \rho_C(\omega)$ one. Note that eq 1 shows that $\varepsilon_{C1\infty} \equiv \varepsilon'_{C1}(\infty)$, a high-frequency-limiting dielectric permittivity contribution but one associated entirely with CSD behavior. The eq 1 transformation from a $k = 0$ model to a $k = 1$ one has also been shown to involve just a simple change in the $k = 0$ DRT.[9,17]

The important effective dielectric constant $\varepsilon_{C1\infty}$ may be expressed as

$$\varepsilon_{C1\infty} = \sigma_{C0}\langle\tau\rangle_{01}/\varepsilon_V \equiv (\sigma_{C0}\tau_{C0}/\varepsilon_V)\langle x\rangle_{01} \equiv \varepsilon_{Ma}\langle x\rangle_{01} \qquad (2)$$

where $\varepsilon_{Ma} \equiv \sigma_{C0}\tau_{C0}/\varepsilon_V$, $\langle\tau\rangle_{01}$ is the mean relaxation time of the $I_{01}(\omega)$ relaxation-time distribution, and $x \equiv \tau/\tau_{C0}$. For the $k = 0$ situation, $\varepsilon_{C0\infty}$ is identically zero, but ε_{C00} is just $\varepsilon_{Ma}\langle x\rangle_0$. The normalized mean, $\langle x\rangle_0$, is unity for a conducting Debye model, and for the more general $k = 1$ $\rho_{C1}(\nu)$ model, $\varepsilon_{C10} = \varepsilon_{Ma}\langle x\rangle_1$.

For the mobile-ion situation with full dissociation, it has been shown that $\varepsilon_{C1\infty}$ is proportional to the ionic number density and to $1/T$, where T is the absolute temperature.[8,9,14] Thus, $\varepsilon_{C1\infty}$ goes to zero as the ionic concentration approaches zero, and eq 2 clearly shows that it is entirely associated with mobile charge, not dipolar effects, contrary to the statement of a reader that such a quantity cannot "arise entirely from mobile ions". Of course, even for pure CSD situations, the bulk dipolar quantity $\varepsilon_{D\infty}$ is always present and greater than 1 in value. Thus, when $\varepsilon_{C1\infty}$ is nonzero, the full high-frequency-limiting dielectric constant is $\varepsilon_\infty = \varepsilon_{C1\infty} + \varepsilon_{D\infty}$ and is never zero. In general, $I_k(\infty) = 0$ for $k =$ D and 0, and so both $\varepsilon'_{DS}(\infty)$ and $\varepsilon'_{0P}(\infty)$ are both identically zero, while for $k = 1$ $\varepsilon'_{1p}(\infty) = \varepsilon_{C1\infty}$, not zero for mobile ion situations.

Interestingly, a reader suggested that a dielectric permittivity such as $\varepsilon'_{0P}(\infty)$ cannot be zero. Such conclusions arise from confusing model results with real data ones. As described above for Debye situations and elsewhere in general,[8,9] such zero values are both appropriate and necessary because a full fitting model requires the addition of the endemic nonzero frequency-independent dipolar quantity $\varepsilon_{D\infty}$ or ε_∞ in parallel with the main dispersive model for $k =$ D and 0 situations. Thus, a free capacitative parameter, C, representing ε_∞ is required in these cases for proper fitting of all dynamic processes present. Because an $\varepsilon_{C1\infty}$ estimate may be calculated directly from estimates of the other parameters present in eq 2, the necessary free parallel fitting quantity in the $k = 1$ case is just $\varepsilon_{D\infty}$. See ref 18 for further discussion of these matters.

2.2. Specific DCD, DC0, DC1 and KD, K0, K1 Dispersive Models. ***2.2.1. The Three Davidson−Cole Models.*** As shown in the previous section, given a dispersive model, it can often be expressed as a $k =$ D dielectric-response model or as a $k = 0$ or $k = 1$ CSD one. The empirical Havriliak−Negami model[19] has been frequently used, especially for DSD data fitting.[1,20] Its normalized form is

$$I_{HN}(\omega) \equiv [1 + (i\omega\tau_{HN})^{\gamma_{CC}}]^{-\gamma_{DC}} \qquad (3)$$

and it reduces to Debye behavior when both shape exponents are fixed at unity, to Cole−Cole (CC) DSD response when γ_{CC} is a free variable and $\gamma_{DC} = 1$, and to Davidson−Cole (DC) response[21,22] when $\gamma_{CC} = 1$ and γ_{DC} is free to vary.

Both the Havriliak−Negami and the Cole−Cole models lead to nonphysical behavior as the frequency tends to zero, however, and so the $k = 0$ form of neither can properly be transformed by eq 1 to $k = 1$ form. Thus, only the three DC models will be considered here. The dielectric-level DC model was originally derived from plausible physical considerations,[21] and such response has also recently been shown to arise from a self-similar fractal assumption, and it is suggested there that the same general type of model derivation should be applicable to ionic hoping as well as to dispersed dipolar rotation.[22] Because the DC model may be used for either DSD or CSD situations, define it as DCD for dielectric response or DC0 or DC1 for conductive-system response. Next, for applications for which $\rho_{C\infty} = 0$, $\rho_{DCk}(\omega) = \rho_{C0}I_{DCk}(\omega)$, with $k = 0$ or 1, and the τ_{HN} of eq 3 is replaced by τ_{C0}. Similarly, its DSD form at the complex dielectric level may be written as $\varepsilon_{DCD}(\omega) = \Delta\varepsilon_{DCD}I_{DCD}(\omega)$, and we shall refer to $\Delta\varepsilon_{DCD}$ as just $\Delta\varepsilon$.

Although up to the present, the eq 1 transformation has only been used for the stretched-exponential Kohlrausch-model situation discussed below, it may be applied to generate a new CSD fitting model, starting from the $I_{DC0}(\omega)$ simplification of eq 3, to obtain a closed-form expression for the DC1-model quantity $I_{DC1}(\omega)$. The three DC-model shape parameters will be denoted γ_{DCD}, γ_{DC0}, and γ_{DC1}. We then find for γ_{DCk} values of 1, 1/3, or 1/6 that $\varepsilon_{C00}/\varepsilon_{Ma}$, $\varepsilon_{C1\infty}/\varepsilon_{Ma}$, and $\varepsilon_{C10}/\varepsilon_{Ma}$ $\langle x\rangle_k$ results are 1, 1/3, or 1/6; 1, 1/3, or 1/6; and 1, 2/3, or 7/12, respectively. The first two series are just the values of γ_{DC0} or γ_{DC1}, while the last ones are given by $(1 + \gamma_{DC1})/2$. The corresponding $k =$ D DSD values of $\varepsilon_{DD0}/\varepsilon_{Ma}$ are the same as those of $\varepsilon_{C00}/\varepsilon_{Ma}$.

2.2.2. The Three Kohlrausch Stretched-Exponential Models. Because no general closed-form analytic expressions are available for the frequency response of these models, one must calculate such response by starting with a known temporal decay or correlation function, $\phi(t)$, and Fourier transforming its negative derivative, $-d\phi(t)/dt$, to the frequency domain. Thus, here one sets $\phi(t)$ equal to Kohlrausch stretched exponential response, $\exp[-(t/\tau_k)^{\beta_k}]$,[8−10,16] where k is either D or 0; the shape parameters β_D and β_0 satisfy $0 < \beta_k \leq 1$; and τ_k is the characteristic stretched-exponential relaxation time. For these two k choices, one formally obtains specific $I_k(\omega)$ response functions, the same except for the immittance level to which they apply.[9] The resulting $\varepsilon_D(\omega)$ DSD response, often just identified as the Williams−Watts (WW)[23] or KWW model, is here named the KD model, and the corresponding CSD $\rho_{C0}(\omega)$ one is designated the K0 model.

The eq 1 transform of K0 $I_0(\omega)$ response leads to specific $\rho_{C1}(\omega)$ CSD response, called the K1 model, and involves a β_1 shape parameter with $0 < \beta_1 \leq 1$.[8,9,14] Although no closed-

form expressions are available for the Kk functions except for a few fractional values of β_k, such as 1/3, 1/2, and 1, they can be calculated very accurately for both simulating and fitting data using the free LEVMW complex-nonlinear-least-squares computer program.[24] It is worth emphasizing that because the K1 model is only indirectly derived from a stretched-exponential Fourier transform, its temporal response, unlike that of the KD and K0 models, is not of stretched exponential form and only reaches it in the limit of long times.[9,14]

For the $k = 0$ and 1 CSD choices, the K0 and K1 models lead to the results $\langle x\rangle_0 = \beta_0^{-1}\Gamma(\beta_0^{-1})$ and $\langle x\rangle_{01} = \beta_1^{-1}\Gamma(\beta_1^{-1})$, where Γ is the Euler gamma function. Given values of β_k and ε_{Ma}, one can then calculate those of ε_{C00} and $\varepsilon_{C1\infty}$ using the expressions given in section 2.1. In addition, it is found that $\varepsilon_{C10} = \varepsilon_{Ma}\Gamma(2\beta_1^{-1})/\Gamma(\beta_1^{-1})$. When $\beta_1 = 1$, 1/3, or 1/6, these results lead to values of $\varepsilon_{C1\infty}/\varepsilon_{Ma}$ (equal to $\varepsilon_{C00}/\varepsilon_{Ma}$ values for the same β choices) and $\varepsilon_{C10}/\varepsilon_{Ma}$ of 1, 6, and 720 and 1, 60, and 332 640, respectively.

Thus, for small β_1 values, the K1 model can lead to exceptionally large effective dielectric constants associated entirely with mobile charge, ones that are much larger than those associated with the DC1 model discussed in section 2.2.1. The K1 $\beta_1 = 1/3$ value is particularly important because for a microscopically homogeneous material whose structure is also temperature independent this value is theoretically predicted to be independent of both temperature and charge-carrier concentration, leading to a semiuniversal response model experimentally found to best fit a wide variety of CSD data.[8,9]

2.3. Composite Fitting Models. A single bulk dispersion model is usually found to be inadequate for good fitting of full immittance data sets because they usually involve more than one physical process, and so a composite model is needed. Such models may include responses in parallel with and/or in series with that of the bulk DSD or CSD model. For easy identification, the designation of such a composite model will be given in the form PB•S, where P includes all elements in parallel with a bulk dispersion model B, and S all the ones in series. For the present work, I shall consider only DCD, KD, K0, and K1 bulk models. For adequate fitting, they all require a specific frequency-independent capacitance in parallel with the model. This capacitance is designated here by C, but its value at the ε level is ε_∞ for the KD, K0, and DCD models, and is $\varepsilon_{D\infty}$ for the K1 and DC1 one, as discussed above.[8,9,18] For the K1 situation, such a composite parallel model is therefore denoted by CK1.

It is often necessary for adequate fitting to include a resistance (resistivity) R in parallel or series with the bulk model. Here, series models of the following types will be used: Debye (abbreviated Deb), DC0, DC1, R, and C_S. C_S represents a series specific capacitance, written as ε_S at the dielectric level. As an example, the RCKD•Deb composite-model name involves the KD bulk response model with R and C (a Debye combination) in parallel with it and with ordinary resistive-level Debye response in series with the parallel combination of all of the other elements.

For a composite model such as RCDCD•DC0, the DCD part is the main DSD bulk model and the CSD DC0 part is in series with it and with the parallel R and C elements. The (R•Deb)-CKD model involves a resistance R and a resistive Debye model in series, with the result in parallel with CKD. Rather than using DSD and CSD elements in series, previous work has often involved a composite model involving two DSD ones in parallel, which may be represented for DCD models by (DCDDCD)•Deb, with the parentheses here enclosing parallel parts. All bulk and composite models discussed here are instantiated in the freely available LEVMW computer program.[24]

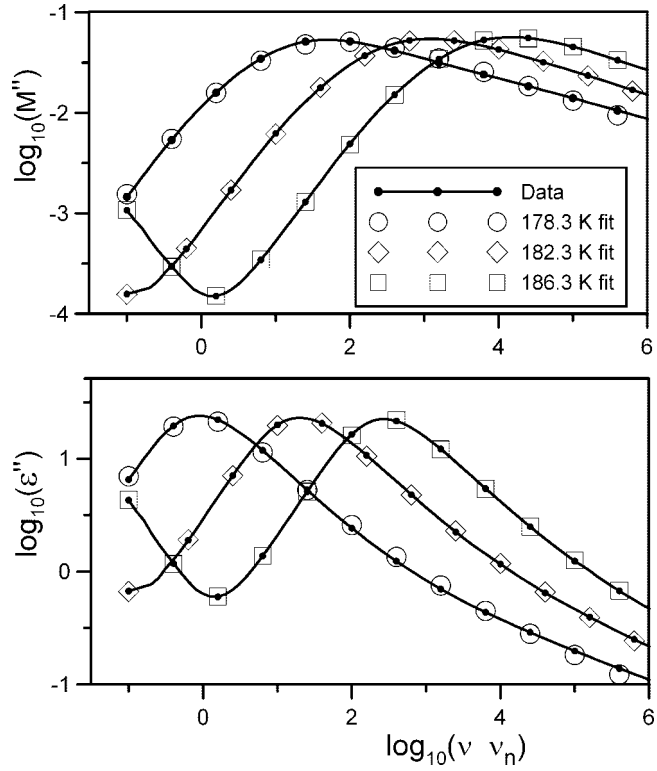

Figure 1. Frequency dependence of NMEC $M''(\omega)$ and $\varepsilon''(\omega)$ data and fits for various temperatures. To avoid overlap and add to clarity, only one out of every six data and fit points are shown, as discussed in section 3.1. The 186.3 and 182.3 K fits involved the composite model CK1•Deb results of rows 2 and 13 of Table 1, while the 178.3 K ones used the CK1•C_s one. Here and elsewhere, ν_n is 1 Hz.

3. NMEC and Glycerol Data and Fit Results

3.1. Representation of NMEC Data and Fit Points. Seven NMEC data sets, kindly supplied by Dr. Ranko Richert, spanned the temperature range from $T = 174.3$ to 186.3 K, and each involved about $N = 71$ data points. No data sets for a wider temperature range were available, but because of the presence of large activation energies, substantial variation in response appeared over the available range. For all seven available NMEC data sets, composite fitting models, including a series response model, were needed to obtain adequate fits of the full complex data. Although plots of the individual real or imaginary parts of full complex data will be shown, all results involved complex nonlinear least-squares fitting,[24] usually at the $\varepsilon(\nu)$ level, with closely comparable ones found for fits with the same model with the data expressed at other immittance levels.

Figure 1 illustrates a powerful approach for depicting data and fit results. The peaked $\varepsilon''(\nu)$ curves of Figure 1 are usually designated as α-relaxation ones associated with dipolar dispersion. Lines are plotted conventionally here by connecting all available data points, but a special procedure is employed to provide information about the adequacy of the fits of individual points to the data. Because this procedure is unconventional for DSD situations, it is described in detail below.

All fits of each data set to a model involved all N data points of the set and led to values of the relative standard deviation of the residuals of a fit, S_F, a global measure of fit. In addition, a measure of the overall uncertainty of parameter estimates, the root-mean-square of the estimated relative standard deviations

TABLE 1: Results of Fitting Complex $\varepsilon(\omega)$ NMEC Data for a Range of Temperatures[a]

row no. and temp (K)	model Lowρ High ρ	$100S_F$ and PDRMS	ρ_{C0} (Ω cm)	τ_{C0} or τ_{D0} (s)	β_k or γ_{DCD}	$\Delta\varepsilon$	ε_∞	$[\rho_{0S}]$ or ρ_{0P} (Ω cm)	τ_{0S} or τ_{0P} (s)	γ_{DCk}	ε_S or ε_{D0}
1	CK0•Deb	2.16	9.15×10^7	1.06×10^{-4}	0.533		3.91	$[4.15 \times 10^{12}]$	23.2	1 F	63.21
186.3		0.011									
2	CK1•Deb	0.791	9.42×10^7	1.48×10^{-7}*	0.228		3.52	$[4.17 \times 10^{12}]$	23.2	1 F	63.01
186.3		0.042									
3	RCDCD	4.64		1.05×10^{-3}	0.544	58.43	3.84	4.17×10^{12}			62.26
186.3		0.012									
4	RCKD•Deb	1.44	9.47×10^7	2.38×10^{-3}*	0.439	59.67*	3.84	$[4.17 \times 10^{12}]$	23.3	1 F	63.11
186.3	L/H	0.134									
5	(R•Deb)CKD	2.75	1.85×10^8	2.68×10^{-4}	0.484	25.16	3.70	4.18×10^{12}	12.6	1 F	63.02
186.3		0.020									
6	RCDCD•Deb	0.846	9.29×10^7	7.47×10^{-4}	0.418	27.92	3.80	$[4.16 \times 10^{12}]$	23.2	1 F	63.08
186.3	L/H	0.024									
7	DC0DCD•Deb	0.512	9.29×10^7	5.68×10^{-4}	0.454	26.20		$[4.16 \times 10^{12}]$	23.2	0.984	63.06
186.3	L/H	0.013									
8	RCDCD•DC0	0.635	8.40×10^6	9.60×10^{-4}	0.530	58.35	4.74	4.15×10^{12}	3.91×10^{-5}	0.846	63.09
186.3	H/L	0.014									
9	CK1•Deb	1.05	3.18×10^8	5.81×10^{-7}*	0.230		3.52	$[1.24 \times 10^{13}]$	70.6	1 F	64.09
184.3		0.050									
10	RCDCD•Deb	1.64	3.12×10^8	3.29×10^{-3}	0.404	30.74	3.75	$[1.24 \times 10^{13}]$	70.3	1 F	64.21
184.3	L/H	0.054									
11	DC0DCD•Deb	0.879	3.13×10^8	2.12×10^{-3}	0.454	28.23		$[1.24 \times 10^{13}]$	70.3	0.983	64.15
184.3	L/H	0.020									
12	RCDCD•DC0	1.07	3.25×10^7	3.39×10^{-3}	0.507	59.44	4.71	1.24×10^{13}	1.22×10^{-4}	0.882	64.15
184.3	H/L	0.016									
13	CK1•Deb	1.20	1.24×10^9	4.00×10^{-6}	0.242		3.52	$[4.82 \times 10^{13}]$	278	1 F	65.25
182.3		0.012									
14	RCDCD•DC0	1.56	1.44×10^8	1.39×10^{-2}	0.484	60.55	4.72	4.34×10^{13}	4.47×10^{-4}	0.907	65.26
182.3	H/L	0.017									
15	CK1•C_S	2.48	5.52×10^9	1.77×10^{-5}*	0.239		3.51				66.33
180.3		0.137									
16	RCDCD•DC0	2.06	7.25×10^8	6.28×10^{-2}	0.462	62.77	4.79	1.425×10^{14}F	1.80×10^{-3}	0.929	67.56
180.3	H/L	0.017									
17	CK1•C_S	4.92	2.94×10^{10}	6.79×10^{-5}*	0.230		3.49*				67.12
178.3		0.308									
18	CDCD•DC0	3.15	4.28×10^9	3.36×10^{-1}	0.435	62.48	4.91		8.38×10^{-3}	0.947	67.35
178.3		0.020									
19	CDCD•DC0	4.54	2.69×10^{10}	2.92	0.398	69.87	5.18		3.87×10^{-2}	0.963	75.04
176.3		0.051									

[a] Here, model identifies the type of bulk conductive or dielectric fitting model used. The various composite fitting models, defined in section 2.3, include elements in parallel and/or in series with the bulk models. The S subscript identifies series-model parameters, and series resistivity quantities are enclosed in brackets here to distinguish them from the parallel ones, denoted by R in the model name and by ρ_{0S} (series fit) or ρ_{0P} (parallel fit) in the table. Values followed by an F are fixed, not free to vary. Fit models including a series Debye part led to the estimates of ε_S shown, and for DCD fits $\varepsilon_{D0} \equiv \varepsilon_\infty + \Delta\varepsilon$. All complex-data fit results shown in Tables 1 and 2 used proportional weighting. The presence of "*" indicates that the relative standard deviation of a quantity is poor and greater than 0.1.

of all free parameters, PDRMS, is also calculated and presented. Although values of these quantities are listed herein, a more detailed and discrete graphical measure will also be employed. Thus, for each data set, only $M \equiv N/R_F$ points are shown, with the value of R_F selected to avoid too close crowding together of plotted individual data points and of their fit estimates. For the NMEC data, a value of R_F of six was employed, allowing about $M = 12$ of the total number of points to appear for each set.

In Figure 1, the M data points shown are plotted as small solid circles connected by lines using all of the data, while the M fit points are shown by open symbols. The size of the open symbols is unrelated to the uncertainty of their fit estimates. For good fits, the centers of the open symbols should fall close to those of the corresponding data ones, avoiding any ambiguity in their placement. In addition, for perfect fits, the open symbols should enclose the solid data points entirely symmetrically, nearly the case for most of those of Figure 1.

Yet consider, for example, the open circle 178 K points of both parts of Figure 1. We see that the centers of the ones at x-axis values of 5 or more fall a significant amount below the centers of their corresponding solid-data points, indicating an imperfect fit for these points. For the two higher-temperature fits, however, the very close agreement between individual data and fit points indicates excellent fits over the entire frequency range shown. The present procedure, which avoids the need for separate residual plots, is much more sensitive and provides more resolution than do the conventional procedures that show the data by solid lines and the fit by either broken lines or by symbols alone. For the present 182 and 186 K cases, such solid and dotted or dashed lines would overlap so closely that they would be indistinguishable.

A reader of an earlier version of the present work characterized the above procedure as confusing and stated that when it is used "some information on the quality of the fits is lost". In fact, because the open fit symbols can appear at any position relative to their corresponding data points, they provide detailed information about the accuracy of both the frequency value and the vertical position of the actual fit estimates, unlike conventional approaches. This reader's further suggestion to use "the

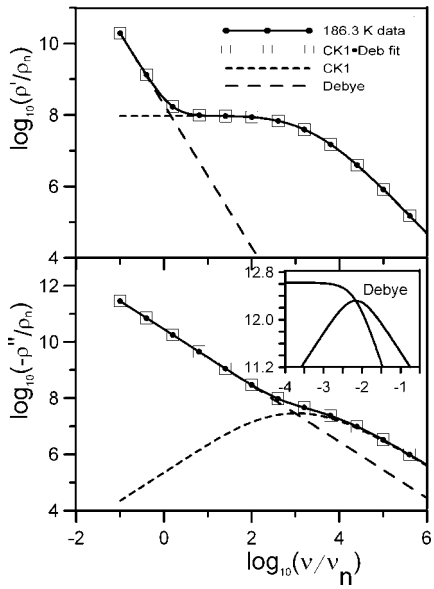

Figure 2. Log−log frequency−response plots of NMEC ρ' and ρ'' 186.3 K data and CK1•Deb-model fits. Also included are the separate CK1 and Debye responses calculated from the model fit parameters, as are low-frequency extrapolated results. The inset shows the calculated full Debye responses at lower frequencies. Here, ρ_n is 1 Ω cm.

standard way of plotting the experimental data as lines and the fits as points" thus provides less, not more, comparative information about the fit.

For both the NMEC and the glycerol data sets, best fits with the CSD CK0 and CK1 models, as in rows 1 and 2 of Table 1, require the series addition of a Debye-response model to take proper account of the low-frequency spur most apparent in the 186.3 K curves of Figure 1. For the bulk $k = 1$ CK1 model, the series composite-model combination is denoted by CK1•Deb, and it is most appropriate to separate its effects at the resistivity level, as shown in Figure 2. The inset, showing extrapolation of the Debye response to lower frequencies, indicates that the lower frequency limit of the data would have had to extend nearly two more decades to show the peak of the $-\rho''$ Debye curve. For temperatures below 182.3 K, the Debye ρ_{0S} quantity becomes too large to estimate adequately within the available fixed-frequency data window, and only the much smaller ρ_{C0} resistivity remains, an intrinsic part of dispersed CSD response.

3.2. Further Graphical and Tabular NMEC Fitting Results. Reference 1 deals primarily with the dielectric behavior of NMEC when confined in the pores of a glass, while the present work involves only bulk NMEC response. Although ref 1 does show some graphical results for the bulk material, no fitting ones are included. Thus, detailed fitting of data for the bulk material is needed and is carried out here.

Figure 1 shows data and fit results for three temperatures, allowing comparison of corresponding $M''(\nu)$ and $\varepsilon''(\nu)$ responses and fits. The first type of plot is usually employed for CSD data and the latter for DSD data. The fit results shown in the figure all used CSD models, but DSD ones have also been employed and are further discussed below. Composite-model parameter estimates for the six largest temperatures are presented in Table 1 and allow direct comparison between fit results for the various CSD and DSD models. In the table, the main dispersive bulk-model parameters for both CSD and DSD models are those listed in columns 4−7. Note that when the γ_{DCk} exponent values of column 11 are set to unity, the DCk model response with $k = 0$ or 1 reduces to Debye response.

In Tables 1 and 2, the quantity $100S_F$ is the percent value of the relative standard deviation of the residuals of a fit and so is an important measure of the adequacy of the fit. Values of three or so are adequate, and those of one or less are excellent. The overall measure of parameter uncertainties, PDRMS, indicates the presence of one or more poorly estimated parameters when it exceeds about 0.05. One should take the values of both of these quality measures into account when evaluating the adequacy and usefulness of a fit.

Fitting results for many different simple and composite models were carried out, and Table 1 shows results for some poor models as well as for more appropriate ones. The row 1, 3, 4, and 5 model fit results were consistently worse than the others at all temperatures and so are not included for the lower temperatures. The (R•Deb) notation in the model designation of row 5 indicates that these quantities are in series and their result in parallel with CKD, and it is interesting that when the R quantity is instead taken in series with the parallel combination of the Deb, C, and KD quantities, the $100S_F$ value increases to 6.2. Although the RCDCD•DC1 model led to most fits as good as or slightly better than the RCDCD•DC0 ones, its results were irregular and thus are not included in the table.

A low-frequency spur, such as that apparent for the two higher temperatures in Figure 1, always appears for partly conducting molecular liquids at frequencies sufficiently below that of the main dispersive response and is usually ascribed to the dc conduction of impurity ions [e.g., refs 2, 25, 26]. As demonstrated by the table results, its effects can be well represented by a resistive Debye-response contribution to the full model in parallel or in series with the bulk response. Yet while inclusion of a single Debye model is sufficient for composite CSD models such as that of row 2, comparison of the row 3 and row 6 $100S_F$ values shows that also for DSD situations a series Debye addition leads to greatly improved fits. Thus, a DSD KD or DCD model alone is inadequate, and both a parallel and a series element need to be added to obtain good fits of data of the present type. The conventional alternative of using two DSD models in parallel is discussed at the end of this section.

Table 1 includes columns with headings identifying two pairs of ρ, τ quantities, the first one for model values as discussed below, and the second for high-resistivity dc conduction processes. For column 4, ρ_{C0} is the resistivity of a dispersion or relaxation fitting model, such as those in rows 1, 2, and 4, while the τ_{C0} or τ_{D0} quantities of column 5 represent the corresponding relaxation time of the model. For DSD models, such as those in rows 5−7, however, one must distinguish between the parallel and series CSD additions to the basic DSD model, here the DCD. These additions may be of either relaxation (RC, Deb) or dispersive (DC0) character, and they may involve either low-value (relaxation or dispersion) or high-value (relaxation only) resistivities. In column 2 of the table, the designations L and H have thus been used to indicate the character of the additional parallel and series parts of a composite model name, reading from left to right.

In column 9, ρ_{0S} and ρ_{0P} represent the high resistivity when it is modeled in series or when it is in parallel. The series Debye responses involve ρ_{0S} in parallel with a specific capacitance, C_S, whose effective dielectric constant is denoted by ε_S and is given by $\varepsilon_S = \tau_{0S}/(\varepsilon_V\rho_{0S})$. For parallel Debye response, the dielectric constant corresponding to the capacitance C is just ε_∞. Thus, for the CK1•Deb CSD model, Deb involves ρ_{0S} and τ_{0S}; the parallel C represents $\varepsilon_{D\infty}$, and $\varepsilon_\infty = \varepsilon_{C1\infty} + \varepsilon_{D\infty}$, but for simplicity, only values of ε_∞ are shown in the tables; and the K1 free parameters are ρ_{C0}, τ_{C0}, and β_1.

TABLE 2: Results of Fitting Complex $\varepsilon(\omega)$ Glycerol Data for Temperatures above $T_g \simeq 185$ K[a]

row no. and temp (K)	model	$100S_F$ and PDRMS	ρ_{C0} (Ω cm)	τ_{C0} or τ_{D0} (s)	β_1 or γ_{DCD}	$\Delta\varepsilon$	ε_∞	$[\rho_{0S}]$ or ρ_{0P} (Ω cm)	τ_{0S} or τ_{0P} (s)	γ_{DCk}	ε_S or ε_{D0}
1	CK1•Deb	2.08	7.83×10^5	1.54×10^{-11}*	0.168		4.00	$[1.22 \times 10^{10}]$	0.0599	1 F	55.63
234		0.134									
2	RCKD•DC1	1.57	2.10×10^5	2.13×10^{-6}	0.624	49.39	6.26	1.05×10^{10}	9.59×10^{-7}	0.169	55.65
234		0.038									
3	RCDCD•DC0	1.83	5.92×10^4*	6.47×10^{-6}	0.570	51.18	4.58	9.09×10^9	3.27×10^{-7}	0.904	55.76
234		0.054									
4	CK1•Deb	1.29	9.13×10^6	1.28×10^{-10}*	0.163		3.90	$[1.53 \times 10^{11}]$	0.815	1 F	60.20
223		0.071									
5	RCDCD•DC0	1.41	8.10×10^5	8.62×10^{-5}	0.520	55.45	4.75	8.82×10^{10}	2.36×10^{-6}	0.945	60.20
223		0.033									
6	CK1•Deb	1.65	1.38×10^8	2.29×10^{-9}*	0.163		3.88	$[2.05 \times 10^{12}]$	11.74	1 F	64.61
213		0.087									
7	RCDCD•DC0	2.56	1.36×10^7	4.20×10^{-4}	0.482	59.68	4.77	1.36×10^{12}	3.20×10^{-5}	0.968	64.45
213		0.041									
8	CK1•Deb	1.66	2.86×10^9	1.52×10^{-7}*	0.173		3.84	$[3.05 \times 10^{13}]$	186.1	1 F	69.01
204		0.091									
9	RCDCD•DC0	2.53	2.72×10^8	3.51×10^{-2}	0.465	63.68	4.77	2.08×10^{13}*	6.12×10^{-4}	0.963	68.59
204		0.062									
10	CK1•Deb	1.88	1.25×10^{11}*	8.76×10^{-6}	0.175		3.87	$[1.72 \times 10^{15}]$*	1.11×10^4*	1 F	73.16
195		0.188									
11	RCDCD•DC0	1.82	9.21×10^9	1.52×10 °	0.486	67.99	4.98	7.59×10^{14}*	2.85×10^{-2}	0.932	72.97
195		0.053									

[a] See the caption of Table 1 for further relevant information.

Parameter identification is somewhat different for DSD models such as those in rows 6−8. For all three, the DCD part of the full model involves the $\Delta\varepsilon$, τ_{D0}, and γ_{DCD} parameters. For rows 6 and 7, Deb again involves ρ_{0S} and τ_{0S}, while for row 8 RC designates Debye response with R and C represented by ρ_{0P} and ε_∞, respectively. The row 7 parallel DC0 involves ρ_{C0}, γ_{DC0}, and a τ_{C0} whose value is not shown in the table but which would lead to an ε_∞ value of about 4.3 were $\gamma_{DC0} = 1$. The row 8 series DC0 model also involves ρ_{C0}, γ_{DC0}, and τ_{C0}, but with its τ_{C0} value actually shown in column 10 in the position of τ_{0S} to save space in the table.

What conclusions follow from the Table 1 results? First, the fits become poorer as the temperature decreases, and for 180.3 K and below no meaningful estimate of ρ_{0S} could be obtained. Its fixed value for row 16 was obtained by extrapolation from higher temperature results, and no reasonable CK1•C_S fits were found for 176.3 K and below. Second, although the CSD CK1-model fit results are of comparable quality to the DSD ones, most of them involve poorly defined estimates of τ_{C0} because the correlation coefficient between τ_{C0} and β_1 is very close to unity, although with the fitting estimate of τ_{C0} taken fixed in a new fit, PDRMS values for such CK1•Deb fits were then comparable to those for the RCDCD•DC0 model.

Third, the CSD ε_S values in column 12 are virtually identical to the $\varepsilon_{D0} = \varepsilon_\infty + \Delta\varepsilon$ ones for the RCDCD•DC0 and DC0DCD•Deb fits. As expected, the estimates of the series and parallel ρ_{0S} and ρ_{0P} dc resistivities were also essentially equal in the temperature range where they could be well estimated. Further, notice that the RCDCD•Deb fit results are inferior to the RCDCD•DC0 ones, and that the RCDCD•DC0 and DC0DCD•Deb fits are comparable. Yet a significant difference between these two is that for the former the DCD equation $\varepsilon_{D0} \equiv \varepsilon_\infty + \Delta\varepsilon$, the low-frequency limit of the dispersive-model response $\varepsilon_D(\omega) = \varepsilon_{D\infty} + \Delta\varepsilon I_{DCD}(\omega)$, leads to values of ε_{D0} in agreement with those of ε_S. This is also the case for the row 3 RCDCD fit, but not for the DC0DCD•Deb one, and its estimates of ε_S actually listed in the table follow instead from the series CSD Deb part of its fits. This behavior suggests that, from a physicochemical viewpoint, the RCDCD•DC0 model is the better one to choose, and so only its results are included for the five lower temperatures.

For CK1•Deb fits, the dispersive response is of CSD character, and one finds that its ε_{C0} values disagree with the ε_S ones associated with these fits. This is strong evidence that even for such CSD fits ε_S values must arise from a DSD dispersive process such as that involving the DCD model, and it thus explains the agreement found with the ε_{D0} estimates obtained from such fits. It is also worth noting that the temperature dependence of the quantities listed in column 12 is quite different from that expected for double-layer capacitative response. If the RCDCD•DC0 choice is indeed the most appropriate one for the present data, it follows that its main dispersive response is of DSD, not CSD, character, just as one would expect from the molecular nature of the material. Nevertheless, the need for complicated DSD composite models for good fitting shows that such fitting requires more than just a single DSD model such as that of row 3.

Of the two Debye-type elements needed in the row 7 and row 8 fitting models, one is in series with the DSD DCD one and one in parallel with it. For both, the Debye-relaxation part (RC or Deb) takes account of the high-resistivity dc response and is necessary, reasonable, and unexceptionable. Yet how can one explain the need for the other DC0 CSD element, one involving dispersed response? First, as discussed above, its presence in series (row 8) seems much more plausible than in parallel (row 7), and it is then always in series with the high-resistivity limiting dc response.

Second, it is interesting that if we replace the DC0-model part of the row 8 composite one by a K1, one obtains a good fit with $100S_F$ and PDRMS values of 0.787 and 0.012, respectively. The K1 parameter estimates are comparable to those in the row 2 CK1•Deb model with a slightly larger value of β_1 of 0.248. Further, the very poorly determined τ_{C0} value in the row 2 fit is now exceptionally well determined. Comparison of these results and those of rows 2, 3, and 8 indicates that while a CSD CK1•Deb model alone is inadequate and physically implausible, the addition of a dispersed CSD model in series with a bulk DSD model, as in that of row 8, is the most appropriate model

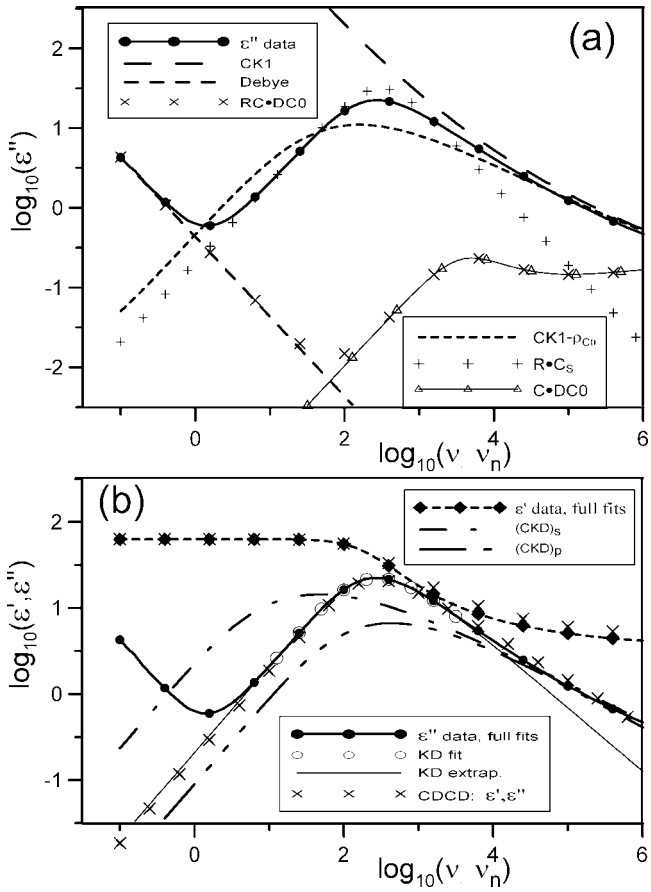

Figure 3. Log−log frequency−response plots of 186.3 K NMEC data and responses of individual parts of the Table 1, row 2 and row 8, composite-model fits. All results shown are for ε'' situations except that identified as ε' in part (b). (a) ε'' CSD responses calculated from the fit-parameter values of the CK1, CK−ρ_{C0}, Debye, and R•C_s parts of full fits, and RC•DC0 and C•DC0 part responses of the full row 8 RCDCD•DC0 fit. (b) DSD responses of the parts of row 4 series RCKD•Deb model and row 5 parallel (R•Deb)CKD-model fits of ε' and ε'' data, and a separate KD-model fit of the peak part of the ε'' response using unity weighting. Its extrapolated low- and high-frequency results are also included. In the figure, the bulk-model DSD parts of the series RCKD•Deb and parallel (R•Deb)CKD fits are denoted by $(CKD)_s$ and $(CKD)_p$, respectively. In addition, the CDCD parts of the response of the full RCDCD•DC0 fit are also included.

choice. We may then interpret the series CSD model as representing the dispersed behavior of bulk mobile impurity ions, of probably a single type, dominant in the mid- to high-frequency range, and the separate very-high-resistivity series response as then arising from partial blocking of these mobile ions at the electrodes.

Figure 3 compares the 186.3 K data with responses calculated from several series and parallel composite-model fits of the full complex $\varepsilon(\omega)$ data. No fit points for the full data sets are shown because in these log−log plots they are indistinguishable from the data points, and, for simplicity, only every sixth data point is shown. The parallel specific capacitance parts of CK1 and CKD models have no effect on $\varepsilon''(\omega)$ response, but their designations are still included here. The estimated fit parameters of the fits were used to calculate the CK1, CK1−ρ_{C0}, CKD, and Debye individual responses shown. The CK1−ρ_{C0} response was calculated by subtracting the effects of ρ_{C0} from that of the CK1 model. Notice especially the close agreement in Figure 3b of the CDCD parts of the row 8 response with the full data at frequencies above about 10 Hz, results much superior to those of the Figure 3a CK1−ρ_{C0} response, a further indication of the appropriateness of a composite DSD model.

The important equality between ε_S and ε_{D0} needs further discussion because ε_S is frequency independent and ε_{D0} is just the low-frequency limit of $-\varepsilon'_D(\omega)$. The Debye response line in Figure 3a shows, however, that its magnitude becomes entirely negligible before the $\varepsilon'(\omega)$ data and its RCDCD•DC0 fit line of Figure 3b begins to decrease from the zero-frequency ε_{D0} limiting value. Thus, the ε_S and ε_{D0} quantities are indeed properly comparable.

We have seen that the addition of a series CSD model, such as the CD0, to the RCDCD model of row 3, as in row 8, leads to greatly improved fits, although at the ε'' level the C•DC0 part of the full response, as shown in Figure 3a, is much smaller over the entire frequency window of the data than is the CDCD ε'' response of Figure 3b. This small effect is consistent with the usual choice of just DSD-model fitting of data where an approximate fit with a single model[4] has often been deemed acceptable, but until the present analysis the possibility of including a series CSD part in the full model has remained unrecognized, and sometimes even three Havriliak−Negami DSD-only fitting functions have been used.[20] It is important to emphasize that, although the C parameter is in parallel with the DCD model for the CDCD composite model, it is in series with the DC0 part of the C•DC0 model. Its effect is thus large for this composite model, and its series addition greatly reduces the size of the C•DC0 ε'' response as compared to that of the DC0 response alone.

The KD model alone has often been used to fit dielectric data, and so for comparison with the present fitting approaches, it was used to fit 26 points around the peak of the $\varepsilon''(\nu)$ data, and its estimated parameters were then used to produce the extrapolated KD lines shown in Figure 3b. Both unity and proportional weighting fits led to an estimate of 0.74 for β_D, comparable to but probably more accurate than the value of 0.76 listed by Ngai for this material using the Fourier transform KD calculation approach,[27] one apparently not involving a least-squares fitting procedure.

As the figure shows, the KD model by itself fails to fit the higher frequency part of the data, an effect invariably characterized as the appearance of an excess wing. Ngai states that the "high-frequency wing is a part of the Johari−Goldstein's β-relaxation hidden under the more prominent α-relaxation." He has also stated that "the presence of the β-relaxation as a peak or shoulder in the loss spectrum preempts an accurate determination of the dispersion of the α-relaxation at higher frequencies and shorter times."[5]

These statements are consistent with probably the most complete previously published description of fitting the frequency-response data for glycerol and other such molecular glass formers,[28] one that involves the use of an all-parallel DSD composite model involving a KD α-response model and a Cole−Cole part to account for excess wing behavior. In contrast, the present composite DSD and series CSD models fit the full range of the NMEC and glycerol data sets excellently without the appearance of an excess wing, and the RCKD•DC0 and RCKD•Deb models yield much smaller β_D values than the KD model alone mentioned above for NMEC,[27] and those for glycerol mentioned in the next section, and those presented in ref 28. Nevertheless, as discussed below, a composite model involving a DSD bulk part has been found somewhat superior for fitting the present data sets than one involving a KD rather than a DSD part.

Although their results are not shown in Tables 1 and 2, many fits involving two DSD models (involving DCD, KD, CC, and Havriliak−Negami model choices) in parallel and the result in series with a Deb one have been carried out for both the NMEC and the glycerol data with similar results for both. For example, for the 186.3 K NMEC data, a RCDCDDCD model, which adds a parallel DCD function to the model of row 3, did not improve the fit, and all three of the additional DCD free parameters were completely uncertain.

On the other hand, fitting with a CDCDDCD•Deb model leads to a $100S_F$ value of 0.50 and to a PDRMS value of 0.053. Even with one more free fitting parameter, this PDRMS value is about 4 times larger than that of the row 8 RCDCD•DC0 model. More importantly, the parameter estimates of this model are inconsistent with all others in rows 5−8, and they lead to an estimate of ε_S much larger than 63. These and similar results show that the conventional choice of fitting with two or more DSD models in parallel can lead to excellent fits that take account of excess wing behavior but to poorly defined and less meaningful parameter estimates as compared to composite models such as the RCDCD•DC0 one.

Finally, the R•C_s curve of Figure 3a is the Debye relaxation response following from just the ρ_{C0} resistivity and the ε_S specific capacitance elements in series. It is remarkable how well it approximates the full response (in the absence of the low-frequency Debye response involving ρ_{0S}) up to 1000 Hz. Nevertheless, it is clear that a composite model involving both dispersed DSD and CSD in series is required to well represent the data and lead to well-defined, plausible, and consistent parameter estimates.

3.3. Glycerol Data and Fitting Results. Adding a dispersive CSD fitting model in series with a DSD one led to over a factor of 7 reduction in the relative standard deviations of the fits for the NMEC results of rows 3 and 8 of Table 1. It is thus important to investigate whether this result is unique for this material or is more general for supercooled glasses. Here, glycerol data sets for five temperatures from 195 to 234 K, kindly provided by Dr. Peter Lunkenheimer, are analyzed. The full complex $\varepsilon(\omega)$ data set responses shown in Figure 2 of ref 4 include very-high-frequency regions of nearly constant loss followed by Boson peaks, but here only regions below the onset of nearly constant loss are included and analyzed. In ref 10, it is shown that similar very wide range CKN data, including the approach to Boson peaks, can be fitted very well, and the models and fit parameters then predict the existence of such peaks, but such added complexity is not needed here.

The Table 2 glycerol fit models are the same as the main NMEC ones of Table 1; the results are mostly similar to the NMEC ones as well; and the quality of the fits decreases as the temperature decreases, although the present data sets are appreciably noisier than the NMEC ones. For the present data, RCKD•DC1 fits were found comparable to and sometimes slightly better than RCDCD•DC0 ones, but except for that of row 2, the latter are presented here to allow direct comparison with those of Table 1. A fit with just the CKD•DC1 composite model led to a $100S_F$ value of 3.44, demonstrating the importance of including the parallel R parameter in the fit model.

As before, we see that most of the CK1•Deb-model τ_{C0} parameter value estimates are poorly determined, and consequently most of the PDRMS CK1•Deb values are larger than those for the RCDCD•DC0 fits. In addition, the estimates of the important ε_S and ε_{D0} quantities are again equal within their uncertainties. Further, the CSD and DSD fit estimates of the ρ_{C0} quantity of column 4 differ appreciably, as they also do for

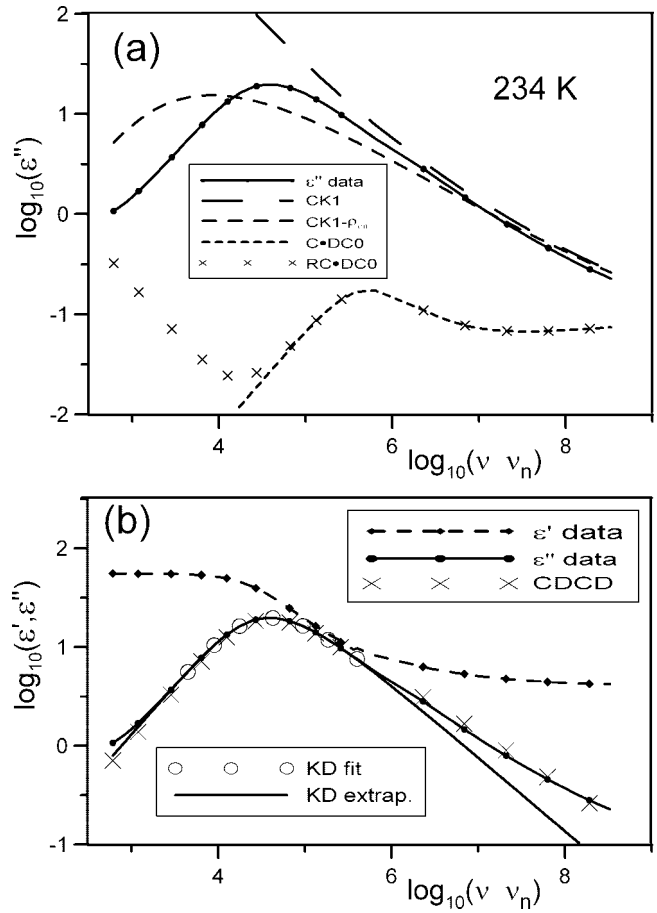

Figure 4. Log−log frequency-response plots of 234 K glycerol data and responses of individual parts of the Table 2, row 1 and row 3, composite-model fits. (a) ε'' CSD responses calculated from the fit-parameter values of the CK1 and CK1−ρ_{C0} parts of the CK1•Deb fit, and RC•DC0 and C•DC0 part responses of the RCDCD•DC0 fit. (b) DSD response of the CDCD part of the row 3 fit of the data, and a separate KD-model fit of the peak part of the ε'' response using unity weighting. Its extrapolated low- and high-frequency results are also included.

the NMEC results. Thus, the present glycerol results confirm the superiority of the RCDCD•DC0 model to the all-CSD CK1•Deb one or to two DSD dispersive models in parallel.

Because the fit results summarized in the present Table 2 are virtually indistinguishable from the data on log−log plots and do not show the excess-wings apparent in Figure 2 of ref 4 or that of Figure 8 of ref 27, in Figure 4 I present only $\varepsilon(\omega)$ data and fit dissections for the 234 K glycerol data set. Here, although the lines connect all data points, for simplicity only every fourth data point is shown and no fit points are included. Except for a shift of the frequency window to higher frequencies, the results are closely comparable to those in Figure 3, demonstrating that the appropriateness of a series combination of a DSD and CSD fitting model is not an isolated phenomenon. In addition, Figure 4b shows the KD-fit curve and its extrapolations obtained by unity-weight fitting of the top part of the $\varepsilon''(\omega)$ data with this model. This fit led to an excess wing and an estimate of $\beta_D \cong 0.747$, larger than the less accurate Ngai one of 0.71.[27]

3.4. Activation Energy Estimates and Relation between τ_{D0} and γ_{DCD} Results. Thermal-activation-energy values for most of the RCDCD•DC0-model free parameter estimates, obtained from Arrhenius fits of the values listed in Tables 1 and 2, are presented in Table 3. These fits used from three to

six values depending on the uncertainties and regularity of the available estimates. Alternative fits of the $\Delta\varepsilon$ values to A + BT and A + B/T showed that the second function led to appreciably better results than the first but both were worse than the Arrhenius activation-energy fit and estimates listed in the table. This was also the case for ε_∞ fits. Because the CSD DC0 model results involve dispersed CSD behavior, activation-energy estimates are provided for ρ_{C0}/T rather than just for ρ_{C0}, less appropriate for this situation.

Although the glycerol ρ_{C0}/T and τ_{C0} activation energy estimates agree, as expected, within one of their standard deviations, this is not the case for the NMEC estimates for unknown reasons. Note that the activation energy estimates for ρ_{C0}/T and ρ_{0P} differ sufficiently for both materials to make it highly improbable that they involve the same process even though both almost certainly entail mobile charges. This is not surprising because the former is associated with dispersed high-frequency response and the latter with charges that are nearly blocked at the electrodes.

It is interesting and probably significant that both the well-defined DSD $\Delta\varepsilon$ activation energy estimates, and the $\Delta\varepsilon$ estimates themselves, are comparable for NMEC and glycerol. In addition, their γ_{DCD} estimates are also comparable. Unlike the γ_{DC0} estimates of column 11, however, the γ_{DCD} values diminish as the temperature decreases, representing greater dispersion. Finally, the glycerol τ_{D0} activation energy estimate listed in Table 3 is poorly defined because the individual τ_{D0} estimated values were somewhat irregular, suggesting possible non-Arrhenius response. Data for more temperature values would be required to resolve this matter using the present parallel-series composite model, but it is significant that fits of glycerol data over a much wider temperature range using two DSD models in parallel show strong non-Arrhenius behavior for the relaxation-time parameter of the KD model used to represent the α relaxation (dispersion) response.[28]

Particularly interesting is the near identity of the activation energy estimates of the dielectric strength parameter, $\Delta\varepsilon$, for NMEC and glycerol. Both materials are good glass formers, and the close agreement of these dielectric-strength activation energy estimates may also be related to their comparable T_g values. In addition, recent theoretical work on supercooled glass-forming liquids is based on a theory of the glass transition[29] involving shear stress and its relaxation, an approach possibly relevant to the above near identity.

This theory predicts a linear relation between the logarithm of τ_P, the value corresponding to the frequency at the peak of the dielectric loss curve, and the $1/\beta_D$ quantity of the KD-model, with β_D calculated from the width of the loss peak.[16] In this work,[29] data for many glass formers were shown to lead to approximately linear relations with a rather abrupt increase in slope as the temperature decreased. All such results were evidently calculated using only three data points and assumed KD response.

It is therefore worthwhile to present somewhat similar results for NMEC and glycerol based on the present full data fits using the RCDCD·DC0 model with γ_{DCD} estimates in place of β_D ones and τ_{C0} estimates rather than τ_P ones. Results are presented in Figure 5 and indeed show appreciable nearly linear regions for both materials, thus generalizing the prediction of ref 29. The glycerol result includes a large increase of slope for its lowest temperature point shown, but the NMEC one appears close to linear over its full range. The data fits become appreciably worse for the two bigger $1/\gamma_{DCD}$ NMEC points, and so error measures are included for them. It appears probable that the NMEC line is actually linear over its full range and that the higher-temperature parts of the lines have nearly the same slope for both materials.

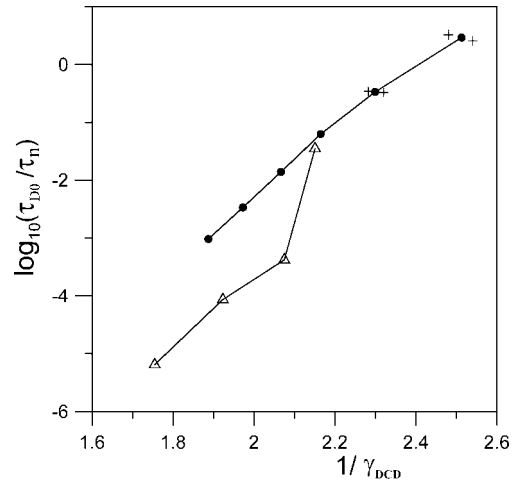

Figure 5. Plots of log (τ_{D0}/τ_n) vs $1/\gamma_{DC0}$ for NMEC (●) and glycerol (Δ) using the RCDCD·DC0 and CDCD·DC0 fit results in Tables 1 and 2. The lines are guides for the eye, and the normalization factor τ_n is 1 s. The + symbols for the two most uncertain NMEC points were calculated using the standard deviation estimates of each of the relevant two fit parameters and define diagonal corners of the rectangular one-standard-deviation error box.

4. Conclusions

It has been shown that good fitting of NMEC and glycerol data sets requires composite models even when the low-frequency Debye-response spur is separately accounted for, and the present results demonstrate that the combination of a bulk DSD dispersive model and a CSD dispersive response function in series yields much better determined parameter estimates for both materials than do two DSD models in parallel. The DSD DCD model here represents the primary dielectric α-dispersion, while a CSD DC0 model in series has been found appropriate to represent high-frequency ionic behavior exhibiting small dispersion and taking the place of what has previously been identified as a parallel DSD Johari−Goldstein β-relaxation hidden under the DSD response, as is well displayed in Figures 3a and 4a. Thus, the presence of such a parallel process in the present data sets seems unlikely.

The equality found between the CSD ε_S estimated values and those of the DSD ε_{D0} ones is convincing evidence that the CSD-only CK1·Deb model is inappropriate and does not properly capture the full dispersive behavior of the data. In contrast, the RCDCD·DC0 model fits the data better and demonstrates the need to account for both DSD dispersive response and CSD dispersive response in series. Comparison of fit results for isothermal data of the present type and that for the same material

TABLE 3: Estimated Activation Energies in eV for the RCDCD·DC0-Model Fit Quantities Listed in Tables 1 and 2

model	ρ_{C0}/T	τ_{C0}	$\Delta\varepsilon$	τ_{D0}	ρ_{0P}	ε_{D0}
NMEC	2.31 ± 0.05	1.97 ± 0.04	0.024 ± 0.001	2.21 ± 0.10	1.72 ± 0.06	0.023 ± 0.001
glycerol	1.20 ± 0.03	1.15 ± 0.05	0.029 ± 0.001	0.9 ± 0.1	1.07 ± 0.04	0.027 ± 0.001

with less ionic impurities should help make entirely clear whether the series CSD response model required here is associated with mobile ions or not. Finally, the near equality found for the small $\Delta\varepsilon$ NMEC and glycerol activation energies suggests significant similarities in their dipolar-dispersion distribution of relaxation times.

Acronyms

C, C_s	Capacitances in parallel or series (C_s) in a composite model
CK1•Deb	K1 model with a capacitance C (representing $\varepsilon_{D\infty}$) in parallel with it and a resistive Debye model in series with the combination
CSD	Conductive-system dispersion involving mobile charges
(DCDDCD)•Deb	Composite model with two DCD models in parallel and the result in series with a resistive Debye model
DCk	Davidson–Cole models for k = D, 0, and 1
Deb	Abbreviation for Debye relaxation model
DRT	Distribution of relaxation times;
DSD	Dielectric system dispersion involving dipoles;
k	k = D, DSD model; k = 0, usual CSD model; k = 1, transformed CSD model
Kk	Kohlrausch stretched-exponential fitting models for k = D, 0, and 1
LEVM	The name of a complex nonlinear least-squares fitting program (ref 24);
NMEC	*N*-methyl-ε-caprolactam;
RC	A resistor, R, in parallel with a capacitor, C;
RCDCD•DC0	Composite model with R and C in parallel with the DSD DCD model and the result in series with the CSD DC0 model.

Acknowledgment. I thank Dr. Ranko Richert for providing NMEC data and Dr. Peter Lunkenheimer for sending me the glycerol data used in this study and for their valuable comments and suggestions. In addition, I am very grateful to the several reviewers of this work whose inputs led to important improvements in it.

References and Notes

(1) Schüller, J.; Richert, R.; Fischer, E. W. *Phys. Rev. B* **1995**, *52*, 15232.
(2) Pissis, P.; Kyritsis, A.; Barut, G.; Pelster, R.; Nimtz, G. *J. Non-Cryst. Solids* **1998**, *235–237*, 444.
(3) Ngai, K. L.; Habasaki, J.; León, C.; Rivera, A. *Z. Phys. Chem.* **2005**, *219*, 47.
(4) Lunkenheimer, P.; Loidl, A. *Chem. Phys.* **2002**, *284*, 205.
(5) Ngai, K. L. *J. Non-Cryst. Solids* **2000**, *275*, 7.
(6) Buchenau, U.; Ohl, M.; Wischnewski, A. *J. Chem. Phys.* **2006**, *124*, 094505.
(7) Brodin, A.; Rössler, E. A. *J. Phys.: Condens. Matter* **2006**, *18*, 8481.
(8) Macdonald, J. R. *Phys. Rev. B* **2005**, *71*, 184307.
(9) Macdonald, J. R. *J. Phys.: Condens. Matter* **2006**, *18*, 629. The word "imaginary" on the third line of p 643 should be replaced by "real". On p 640, next to the bottom line, replace $\rho_0\varepsilon_{D\infty}$ by $\rho_0\varepsilon_V\varepsilon_{D\infty}$.
(10) Macdonald, J. R. *J. Phys. Chem. B* **2007**, *111*, 7064.
(11) Johari, G. P.; Pathmanathan, K. *Phys. Chem. Glasses* **1988**, *29*, 219.
(12) Stickel, F.; Fischer, E. W.; Richert, R. *J. Chem. Phys.* **1995**, *104*, 2043.
(13) Scher, H.; Lax, M. *Phys. Rev. B* **1973**, *7*, 4491.
(14) Macdonald, J. R. *Solid State Ionics* **2002**, *150*, 263.
(15) Macdonald, J. R. *Braz. J. Phys.* **1999**, *29*, 332.
(16) Moynihan, C. T.; Boesch, L. P.; Laberge, N. L. *Phys. Chem. Glasses* **1973**, *14*, 122.
(17) Macdonald, J. R. *J. Non-Cryst. Solids* **1997**, *212*, 95. The symbol "σ" should be removed from the right end of eq 12.
(18) Macdonald, J. R. *J. Appl. Phys.* **2004**, *95*, 1849.
(19) Havriliak, S.; Negami, S. *J. Non-Cryst. Solids* **1994**, *172–174*, 297.
(20) Corezzi, S.; Capaccioli, S.; Lucchesi, M.; Rolla, P. A. *J. Phys.: Condens. Matter* **1999**, *11*, 10297.
(21) (a) Davidson, D. W.; Cole, R. H. *J. Chem. Phys.* **1951**, *19*, 1417. (b) Davidson, D. W. *Can. J. Chem.* **1961**, *39*, 571.
(22) Nigmatullin, R. R.; Ryabov, Y. E. *Phys. Solid State* **1997**, *39*, 87.
(23) Lindsey, C. P.; Patterson, G. D. *J. Chem. Phys.* **1980**, *73*, 3348.
(24) (a) Macdonald, J. R.; Potter, L. D. *Solid State Ionics* **1987**, *23*, 61. (b) Macdonald, J. R. *J. Comput. Phys.* **2000**, *157*, 280. The newest WINDOWS version, LEVMW, of the comprehensive LEVM fitting and inversion program, as well as the MS-DOS version, may be downloaded at no cost from http://jrossmacdonald.com. It includes an extensive manual and executable and full source code. More information about LEVM is provided at this website.
(25) Molak, A.; Paluch, M.; Pawlus, S.; Klimontko, J.; Gruszka, I. *J. Phys. D: Appl. Phys.* **2005**, *38*, 1450.
(26) Bielowka, S. H.; Psurek, T.; Ziolo, J.; Paluch, M. *Phys. Rev. E* **2001**, *63*, 062301.
(27) Ngai, K. L. *J. Phys.: Condens. Matter* **2003**, *15*, S1107.
(28) Ngai, K. L.; Lunkenheimer, P.; Leon, C.; Schneider, U.; Brand, R.; Loidl, A. *J. Phys. Chem.* **2001**, *115*, 1405.
(29) Trachenko, K.; Roland, C. M.; Casalini, R. *J. Phys. Chem. B* **2008**, *112*, 5111.

JP805535W